



# Cement-based sensors with carbon fibers and carbon nanotubes for piezoresistive sensing

Faezeh Azhari\*, Nemkumar Banthia

University of British Columbia, Department of Civil Engineering, Vancouver, BC, Canada V6T 1Z4

## ARTICLE INFO

### Article history:

Received 27 December 2010  
Received in revised form 6 April 2012  
Accepted 10 April 2012  
Available online 21 April 2012

### Keywords:

Structural health monitoring  
Self-sensing materials  
Cement-based sensors  
Carbon fibers  
Carbon nanotubes  
Electrical resistivity  
Piezoresistivity

## ABSTRACT

Electrically conductive cementitious composites carrying carbon fibers and carbon nanotubes were developed and their ability to sense an applied compressive load through a measureable change in resistivity was investigated. Two types of cement-based sensors, one with carbon fibers alone and the other carrying a hybrid of both fibers and nanotubes, were considered. Direct comparisons were also made with traditional strain gauges mounted on the sensor specimens.

Sensing experiments indicate that under cyclic loading, the changes in resistivity mimic both the changes in the applied load and the measured material strain with high fidelity for both sensor types. The response, however, is nonlinear and rate dependent. At an arbitrary loading rate, the hybrid sensor, containing a combination carbon fibers and nanotubes, produced the best results with better repeatability.

© 2012 Elsevier Ltd. All rights reserved.

## 1. Introduction

Structural health monitoring (SHM) has the role of continuously monitoring and evaluating the state of structural systems. SHM systems are able to provide real-time data on the condition of structures using a network of sensory devices measuring parameters like displacement, strain, temperature, etc. This information will then help engineers and owners in the timely detection of anomalies in the structure's performance, leading to informed decisions on its maintenance.

Often described as smart (self-monitoring) structural materials, conductive cement-based materials have recently become the subject of a number of studies [1–22], proposing their use as strain sensors in the SHM of concrete structures. As opposed to other sensors, their cementitious nature would allow them to develop a natural bond when integrated into the parent structure. These sensors would function based on the principle of piezoresistivity, defined as the dependence of electrical resistivity on the applied strain [23].

In order to obtain a piezoresistive cement-based material, a conductive substance, usually carbon fibers, is incorporated into a cementitious matrix. Other materials, such as carbon black or carbon nanotubes, may also be used as the conductive phase [1–3]. These conductive materials can enhance the electrical

conductivity of cementitious composites by around two orders of magnitude [3].

Carbon fibers (CFs) are of particular interest as they are less costly and not only improve the conductivity but also enhance the mechanical properties such as fracture toughness and strain capacity [4–12]. The high electrical conductivity of some fiber reinforced cementitious composites has been utilized in several innovative ways to characterize internal structure, performance and damage. Torrents et al. [18], for example, combined the use of Impedance Spectroscopy (IS) and Digital Image Correlation (DIC) to separate the fiber and matrix effects and used this technique to study crack propagation processes in fiber reinforced concrete. The technique relies on the fact that at low frequencies the matrix dominates the electrical performance and at higher frequencies the fibers control the electrical response. Concrete containing short carbon fibers has also proven to be highly effective in traffic monitoring as well as for weighing-in-motion [19] and in monitoring the deformation and crack creation in asphalt pavements [20].

Carbon nanotubes (CNTs), with their extraordinary mechanical properties and extremely high aspect ratios, can also be effectively used as ideal reinforcing fibers for stronger and tougher cement and concrete materials [22,24,25]. Also, these nanoscale materials can potentially act as fillers, refining the pore size distribution in the matrix and decreasing the porosity of the composite, which in turn will help restrain crack growth and propagation.

One promising approach in the development of cement-based sensors is the use of CNT as the conductive substance. If properly

\* Corresponding author. Address: Ausenco Sandwell, 855 Homer Street, Vancouver, BC, Canada V6B 2W2.

E-mail address: [fazhari@gmail.com](mailto:fazhari@gmail.com) (F. Azhari).

dispersed, the addition of CNT to cement paste can lead to a notable increase in electrical conductivity. Li et al. [22] have successfully been able to confirm that the sensitivity of CNT reinforced composites to cyclic compressive loading. In this study, the possible hybridization of CF and CNT for use in cement-based sensors is explored.

## 2. Experimental program

### 2.1. Materials and mixes

Two sets of cement-based sensor samples with mix proportions given in Table 1 were prepared; those carrying carbon fibers alone (CF sensors) and those that carry a combination of carbon fibers and nanotubes (hybrid sensors). The samples were cylindrical, 50.8 mm in diameter and 100 mm long. Four copper electrodes were attached to the samples with silver paste to allow for four-probe resistance measurements (see Fig. 1). The specimens were de-molded after 24 h and then cured for at least 2 months before testing. Typical scanning electron microscope (SEM) images of the CF and CNT specimens are displayed in Fig. 2. At least two samples from each sensor type and an average of five areas for each specimen were observed. In the CF sensors, the fibers were well dispersed regardless of the area observed. CNT, on the other hand, formed clusters; Fig. 2b shows the bridging effect in one of the clusters.

Coal-tar pitch-based carbon fibers with specifications given in Table 2 were used in both sensor samples. These fibers are collated and therefore relatively easy to mix at very high volume fractions. Multi-walled carbon nanotubes (MWCNTs) with specifications given in Table 3 were used in the hybrid sensor specimens.

A fiber volume fraction of 15% was chosen with regards to a previous study [3] conducted to assess the electrical properties of composites with a range of fiber dosages. According to the results, a volume fraction of 15%, which is well above the percolation threshold and provides a near two order-of-magnitude drop in resistivity, is the optimum CF content for sensing purposes because its base-line resistivity stabilizes after a certain curing period and is much less affected by moisture and chloride. In the hybrid sensors, nanotubes were added at an amount of 1% by volume.

Mixing high CF contents proved challenging and hence a high shear mixer was used throughout with a specially designed fiber separation, dispersion and mixing sequence. Methylcellulose was added to the mix along with a defoamer to help disperse the fibers. In order to achieve the desired water to cementitious material ratio of 0.3, a polycarboxylate-based superplasticizer was used.

In the hybrid samples, achieving a good dispersion became even more difficult because CNT have a strong tendency to cluster due to van der Waals forces [25]. In this study, two dispersion methods were used. One method was to disperse the MWCNT in a water-superplasticizer mixture by means of sonication before they were added to the rest of the material. The superplasticizer was added

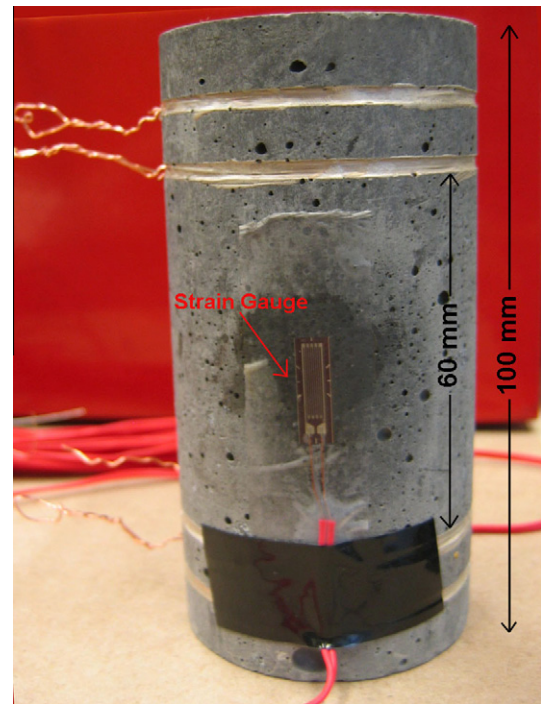


Fig. 1. Sensor specimen.

to act as a surfactant. The other method was to dry mix the MWCNT and silica fume with a high speed hand mixer. In both cases the amount of water and superplasticizer required to achieve a workable mixture was more than that of CF samples. This can be explained by the extremely high specific surface area (233 m<sup>2</sup>/g) of MWCNT. The two dispersion methods produced similar resistivity values.

It was postulated that adding nanotubes to the sensors would provide an effective bridging of existing pathway for electrical conduction and the synergy between the fibers and nanotubes would proffer superior electrical conductivity and piezoresistive properties. However, comparing the average base-line resistivity values for the CF and hybrid sensors (Table 1) a 10% improvement in conductivity was noticed as a result of hybridizing CF with MWCNT, which is not as significant as expected.

CNT are known to have diameters similar in scale to the layers in calcium-silicate-hydrate (C-S-H), and therefore when incorporated in a cementitious matrix, CNT are enwrapped by C-S-H [24–26]. It is suggested by some researchers [25] that these C-S-H layers prevent contact between the nanotube bundles and thwart the anticipated increase in conductivity.

Another reason for not achieving much higher conductivity with CNT may be that the cement used was not fresh enough and had hydrated into clumps. These clumps are much larger than

Table 1  
Mix proportions.

Name	Average base-line resistivity ( $\Omega$ -cm)	Volume fraction of CF and MWCNT	SF/cement (by weight)	W/CM SP (% of CM)	MC (% of CM)	Defoamer (% of CM)	
CF sensor	413	15% CF	0.2	0.3	1.2	0.4	0.2
Hybrid sensor	371	15% CF and 1% MWCNT	0.2	0.4	2	0.4	0.2

CF: carbon fiber.

MWCNTs: multi-walled carbon nanotubes.

SF: silica fume.

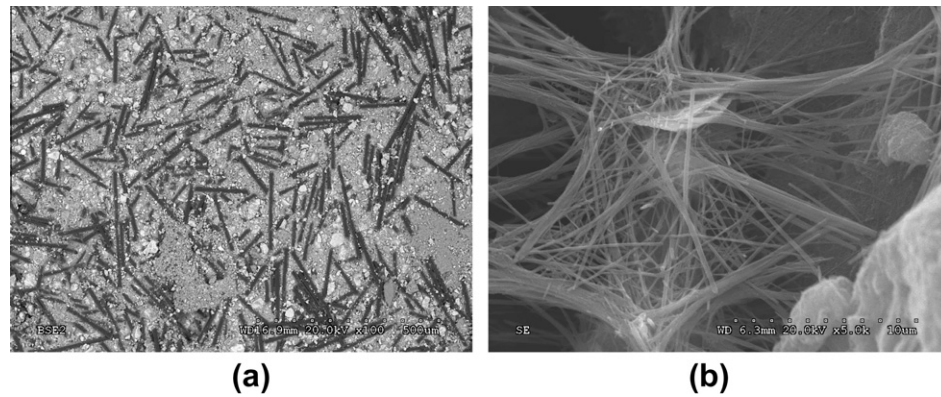
W: water.

CM: cementitious material (type GU cement and silica fume).

SP (% of CM): superplasticizer as a percentage of cementitious material.

MC (% of CM): methylcellulose as a percentage of cementitious material.

Defoamer (% of CM): defoamer as a percentage of cementitious material.

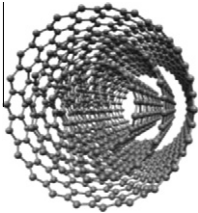


**Fig. 2.** SEM Images of CF and MWCNTs in a cementitious matrix, (a) CF in cement composite @ 100× magnification; (b) MWCNT bridging hydration products @ 5000× magnification.

**Table 2**  
Properties of carbon fibers (CFs).

Length (mm)	Diameter (μm)	Carbon content	Specific gravity	Tensile strength (GPa)	Electrical resistivity (Ω-cm)
6	11	>99%	2.12	2.6	$2.3 \times 10^{-4}$

**Table 3**  
Properties of multi-walled carbon nanotubes (MWCNTs).

Geometry	Length (μm)	Outer diameter (nm)	Inside diameter (nm)	Purity	Specific gravity	Tensile strength (GPa)	Electrical resistivity (Ω-cm)
	10–30	10–20	3–5	>95 wt.%	≈1.5	≈100	<10 <sup>-2</sup>

nanotubes and are not penetrable, thus create regions with no CNT [27]. The most prominent reason, however, is that the dispersion techniques used were not efficient enough. Several other CNT dispersion methods, promising better results, have recently been developed by other studies: implanting or growing CNT on non-hydrated cement particles; using functionalized CNT; using fine-grain cement; and co-grinding [24,25,27].

## 2.2. Sensing measurements

Sensor specimens were subjected to compressive loading using a 150 kN closed-loop MTS loading machine. Two LVDTs, one on either side of the specimen, were used to measure displacement. For comparison purposes, 10 mm foil strain gauges were also attached to either side of the specimen. The corresponding electrical resistance was, simultaneously, measured using an Agilent 4263B LCR meter at 100 kHz frequency. Since a direct current (DC) measurement of electrical resistance is technically difficult and problematic due to the polarization effects [27–29], resistance measurements were made using alternating current (AC). The four-probe technique was employed whereby current flows between the two outer electrodes and the voltage between the inner electrodes is measured.

Acquired load, displacement, strain and resistance data were transferred to a PC equipped with NI LabVIEW platform. The experimental setup is shown in Fig. 3. To take into account the nature and geometry of the sensors, the resistance measurements were

converted to electrical resistivity ( $\rho$ ) calculated as resistance per unit length:

$$\rho = R \frac{A}{\ell} \quad (1)$$

where  $\rho$  is the electrical resistivity (Ω cm),  $R$  the electrical resistance (Ω),  $A$  the cross-sectional area (cm<sup>2</sup>), and  $\ell$  is the length between the inner electrodes (cm).

A set of preliminary experiments were conducted on the CF sensors to obtain the maximum load capacity of the specimens. The response of the CF sensors to cyclic loading with various load amplitudes was also assessed. Next, the response of CF and hybrid sensors to cyclic loading with a chosen amplitude of 30 kN were compared.

## 3. Results and discussion

A maximum load capacity of around 110 kN was obtained through monotonic compressive loading of three CF samples. Through this experiment, electrical resistivity was also monitored and the results are given in Fig. 4a. The resistivity values decreased from over 400 Ω-cm to less than 200 Ω-cm with the increase in load, but not in a linear fashion. The entire response was non-linear, for a linear change in load with time.

The rate at which the resistivity decreased was higher initially, but gradually lowered as the loads surpassed 60 kN, perhaps because internal micro-cracking was occurring. After that, the



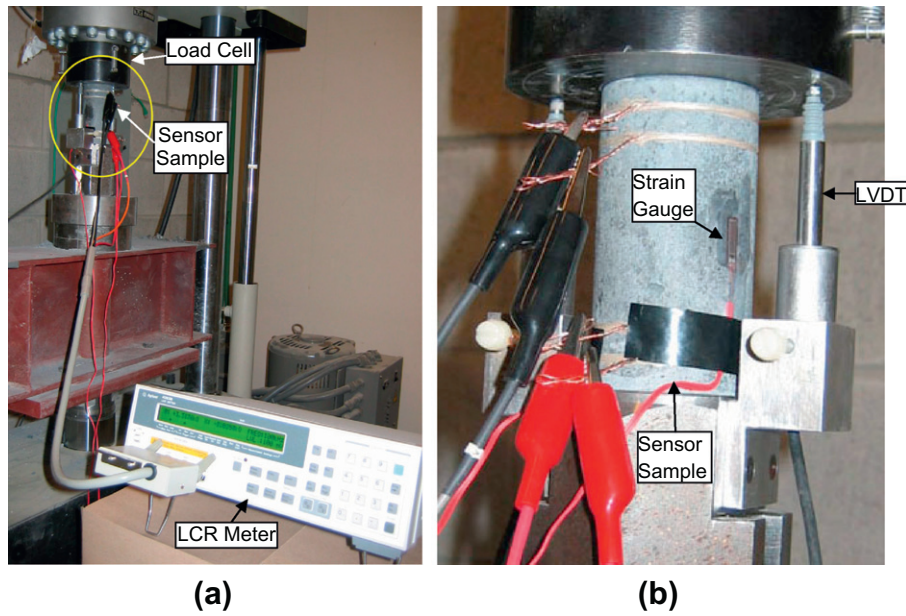


Fig. 3. Compressive sensing, (a) setup; and (b) close-up of specimen.

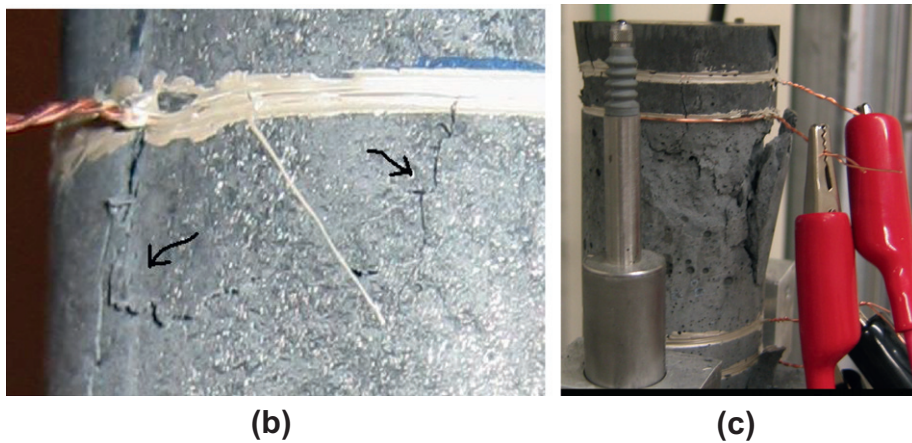
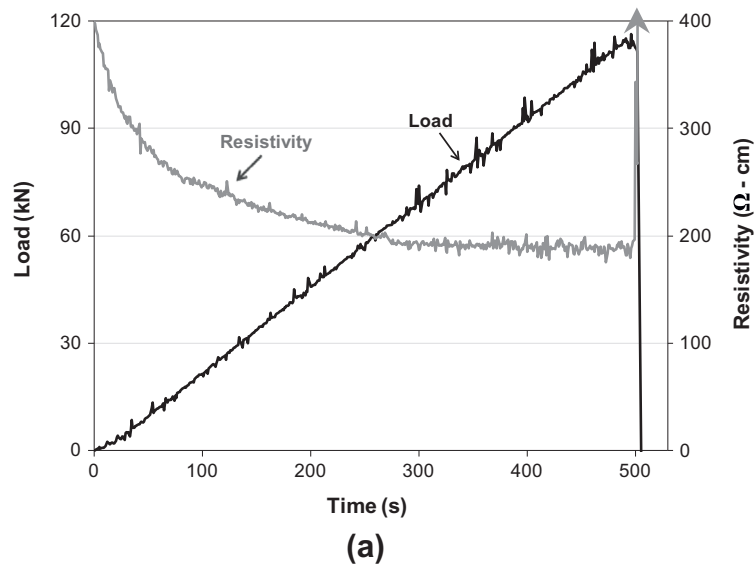


Fig. 4. (a) Response of CF cement-based sensors to monotonic compressive loading; (b) appearance of cracks; and (c) failure.

response started to flatten even more due to the abundance of micro-cracks and eventually visible macro-cracks started to appear (see Fig. 4b), implying that the material became even less sensitive to load. As the load inched toward towards the ultimate capacity, and the cracks became larger, the resistivity values changed direction and increased considerably to reach just about 345  $\Omega$ -cm and then suddenly soared almost tenfold to about 3500  $\Omega$ -cm, indicating failure (Fig. 4c).

To further assess the piezoresistive quality of the CF sensors, a series of cyclic loading tests with various load amplitudes were performed. For the cyclic experiments, the applied load was compared against fractional change in resistivity (FCR):

$$FCR = \frac{\rho_t - \rho_0}{\rho_0} \quad (2)$$

where  $\rho_t$  is the electrical resistivity at time  $t$  during the tests; and  $\rho_0$  is the electrical resistivity at the beginning of the test (prior to loading).

Fig. 5 displays the response of CF sensors to cyclic loading with different amplitudes. The loading rate was set so that each cycle took 500 s, regardless of amplitude, leading to loading rates of 0.01 kN/s, 0.02 kN/s, 0.04 kN/s, 0.06 kN/s and 0.12 kN/s for 5 kN, 10 kN, 20 kN, 30 kN and 60 kN load amplitudes, respectively. Notice that the electrical resistivity of the sensors varied distinctly in response to the applied loading. During each loading cycle, the resistivity values decreased with an increase in compressive load, resulting in a negative FCR, and then increased to the initial value when the unloading branch of the cycle took place.

Cement-based sensors do not respond in a linear fashion, but there may be a unique nonlinear correlation between resistivity values and load/strain that can be used for calibration. In Fig. 6, the loading branch of a single cycle is plotted for the five different loading rates. It appears that the response is not only nonlinear, but also rate-dependant.

Hyperbolic trend lines were fitted to the data points in Fig. 6 by minimizing the sum of squared errors. The general equation for these curves is:

$$FCR(t) = \frac{At}{1 + Bt} \quad (3)$$

where  $t$  is the time (s); and  $A$  and  $B$  are constants.

The constants,  $A$  and  $B$ , were then plotted against loading rate; revealing almost linear correlations. Therefore, given the loading rate, these constant values can be determined and used in monitoring load or strain. Further research is required to confirm this relationship and to find out whether it can be extrapolated for very low and very high loading rates, representing creep and impact, respectively.

In the next round of experiments, the samples, now equipped with two strain gauges, were cyclically loaded to an amplitude of

30 kN (chosen to represent approximately 30% of the compressive capacity) at a rate of 0.06 kN/s. Fig. 7a and b juxtapose the variation in FCR, in response to the cyclic load and measured strain. The non-linear trait of the cement-based sensors produces a domed response as opposed to the sharp response of the conventional strain gauges. The maximum FCR values are in the order of 25% and correspond to about 1000 micro-strains.

A very subtle drift is traceable in the resistivity pattern, which could be a result of temperature change. Temperature variation is known to influence resistivity measurements from the cement-based sensors. In a previous study [3] the response of these sensors to temperatures in the range of  $-15^\circ\text{C}$  to  $60^\circ\text{C}$  was investigated. Resistivity measurements were made at fixed time intervals during a 5-h long full cycle of temperature variation. According to the results, electrical resistivity is inversely related to temperature in a reversible manner, decreasing with the increase in temperature and vice versa, at a rate of approximately  $29 \Omega/\text{cm}/^\circ\text{C}$ . Back-tracking this minor thermal hysteresis using the suggested correction rate, it was found that the drift could be explained entirely by a temperature change of less than  $0.4^\circ\text{C}$  after four cycles of compressive loading which is entirely possible.

Fig. 7c shows the FCR-load correlation for the four cycles of loading. The scatter in the results is quite large; for a given load, the FCR response could have error margins of  $\pm 0.08$  to  $\pm 0.05$ . Unless this lack of accuracy is resolved, through better sensor preparation techniques and materials, these sensors may not be practical for accurate condition monitoring.

Further, to get a sense of how sensitive the cement-based materials could be, FCR and strain values for a single cycle of loading are plotted against each other in Fig. 7d. The initial part of the response, offers a gauge factor (defined as fractional change in resistance per unit strain Eq. (4)) of approximately 445, which is well above that of conventional strain gauges. However, there are two issues to keep in mind: one is that the gauge factor is also rate dependant and may be much smaller for very low loading rates, and the second is the lack of accuracy and repeatability observed in Fig. 7c. In view of these concerns, the apparently high gauge factor is not really of much benefit.

$$\text{Gauge factor} = \frac{\Delta R/R_0}{\varepsilon} = \frac{\Delta \rho/\rho_0}{\varepsilon} = \frac{FCR}{\varepsilon} \quad (4)$$

where  $\Delta R$  (or  $\Delta \rho$ ) is the change in resistance (or resistivity);  $R_0$  (or  $\rho_0$ ) the unstrained resistance (or resistivity);  $FCR$  the fractional change in resistivity; and  $\varepsilon$  is the strain.

It is probable that the scatter in the FCR response is due to the inconsistencies in the dispersion pattern of CF in the cementitious matrix throughout the sample volume. Although the CF are relatively well-dispersed (as shown by SEM, Fig. 2a), their distribution is not completely homogenous; this leads to different resistance measurements each time the sample is loaded, depending on the load path.

If in fact CNT can bridge the existing pathways between the CF and create a more uniform conduction path, regardless of how the load is distributed, then having CNT in combination with CF could very well help increase the accuracy and repeatability of cement-based sensors. This hypothesis was put to test with hybrid samples containing 15% CF and 1% MWCNT; Fig. 8 is the equivalent of Fig. 7, only this time showing the results from the hybrid sensors.

Once again, the variation in FCR effectively follows the load and strain patterns, validating the piezoresistive quality. Comparing Figs. 7c and 8c, one can quite clearly observe the improvement in repeatability and accuracy: the error margins of the hybrid sensors are roughly  $\pm 0.05$  to  $\pm 0.02$ , which are about half those of sensors only carrying CF. The gauge factor for the hybrid sensors at the specific loading rate of 0.06 kN/s (see Fig. 8d) is comparable to that of the CF sensors.

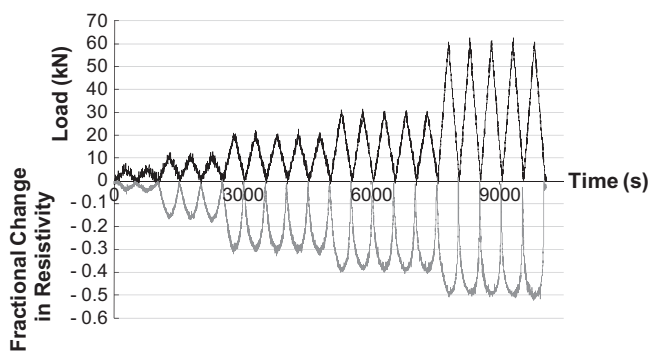


Fig. 5. Response of CF cement-based sensors to cyclic compressive loading.

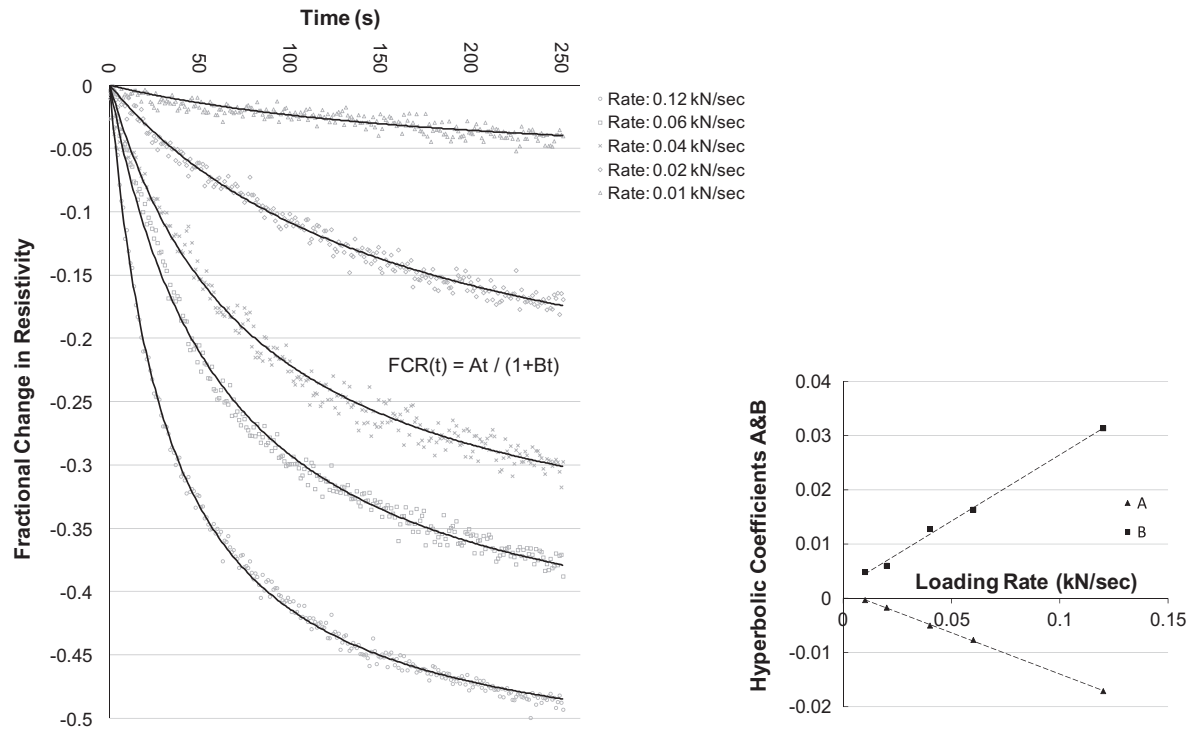


Fig. 6. Rate dependence of cement-based sensors to cyclic compressive loading.

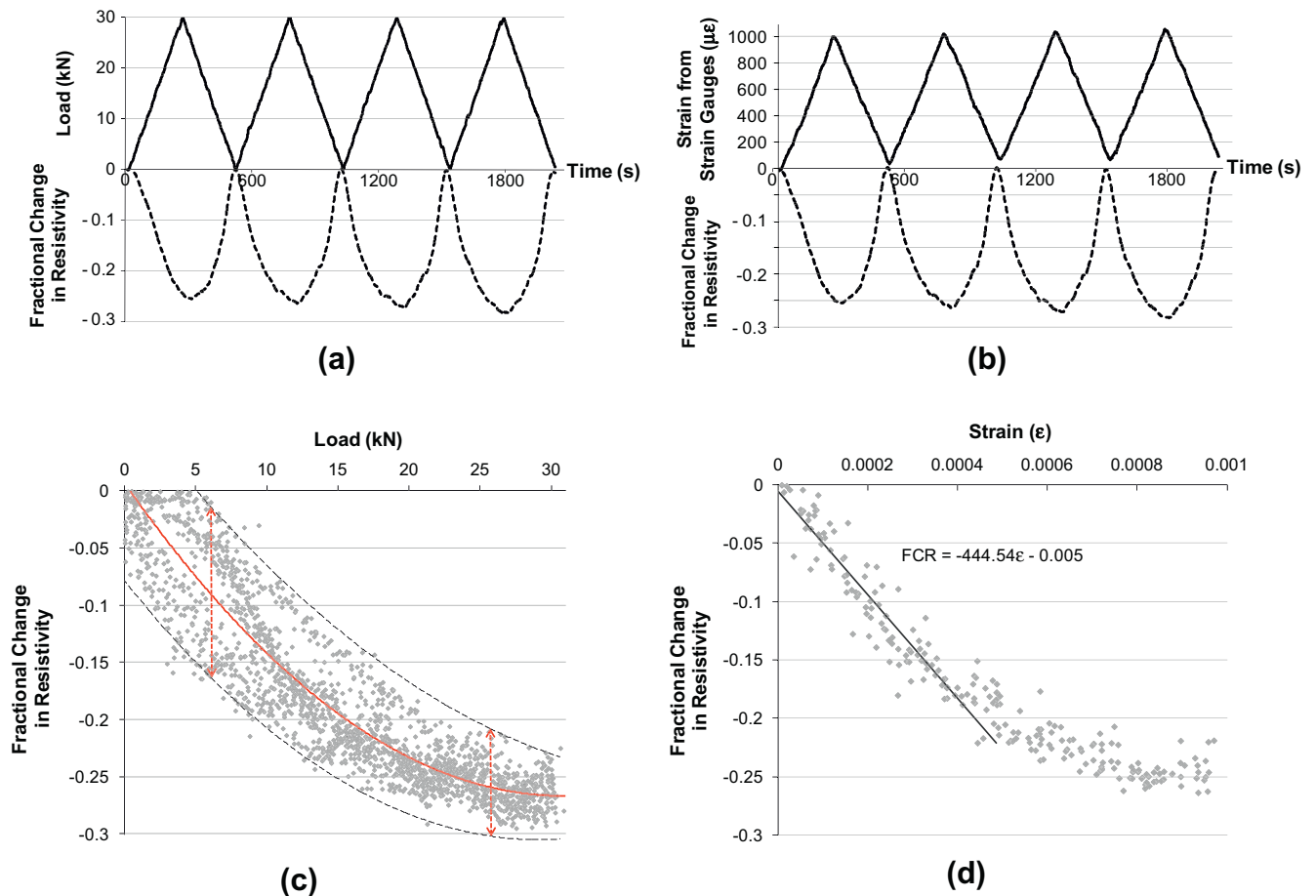
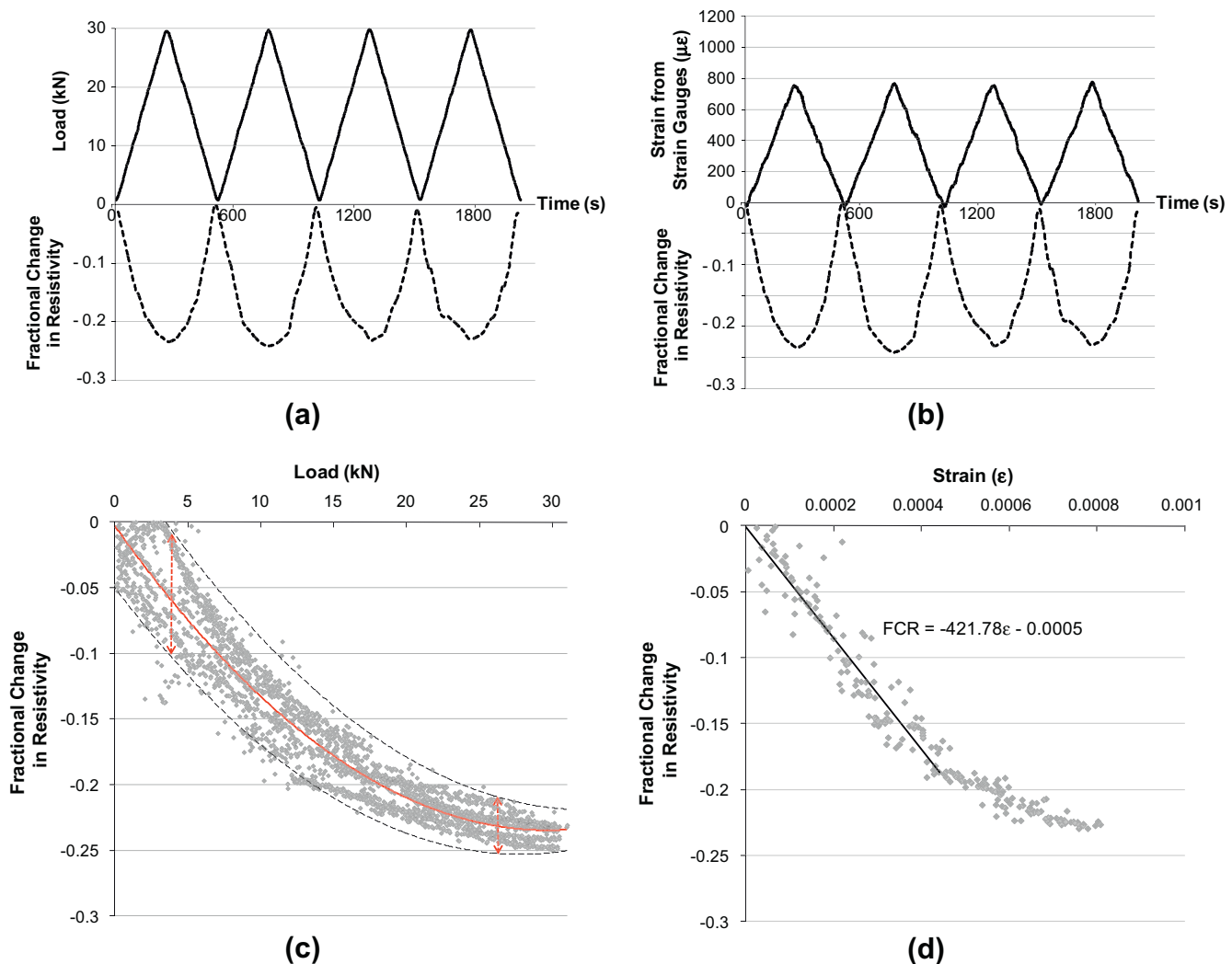


Fig. 7. Cyclic compression response of 15% CF sensor, (a) FCR vs. load; (b) FCR vs. traditional strain; (c) FCR – load correlation; and (d) FCR – strain correlation.



**Fig. 8.** Cyclic compression response of hybrid (15% CF + 1% MWCNT) sensor, (a) FCR vs. load; (b) FCR vs. traditional strain; (c) FCR – load correlation; and (d) FCR – strain correlation.

The superior performance of the hybrid sensors can be attributed to the fact that CNT help close the gaps in the CF conduction path and provide the sensor with a more homogenous quality in terms of electrical properties. That is to say, if the sensor is repeatedly loaded with the same rate, the measured resistivity value at a certain load point would be more or less the same each time.

The error margins could be significantly reduced by employing more effective CNT dispersion techniques, as well as utilizing a better quality control system to ensure the materials and fabrication methods are not adversely affecting the sensor properties. It is fair to assume that had the CNT been dispersed in a more uniform way, not forming any clusters, the hybrid sensors would have exhibited even more superior results.

#### 4. Conclusions

Carbon fiber and carbon nanotubes significantly increase the electrical conductivity of cementitious materials. These conductive cement-based materials are also piezoresistive and can thus produce excellent sensors. The sensor material responds well to an applied compressive strain by depicting a reduction in its resistivity, and this applies to both monotonically and cyclically applied strain fields. Creation of microcracks is signified by a steady increase in the resistivity which then changes to a sudden upsurge when

microcracks coalesce and failure occurs. Thus, in addition to strain sensing, these materials can sense microcracking and failure.

Although the resistivity of cement-based sensors varies in tandem with the applied stress, their response is both nonlinear and rate-dependent. However, given the loading rate, the imposed material strains can be predicted from fractional changes in the sensor resistivity through a unique nonlinear calibration curve. For an arbitrary loading rate, the hybrid sensors, containing a combination of carbon fibers and carbon nanotubes, provide better quality signal, improved reliability and increased sensitivity over sensors carrying carbon fiber alone.

#### References

- [1] Ou J, Han B. Piezoresistive cement-based strain sensors and self-sensing concrete components. *J Intell Mater Syst Struct* 2009;20(3):329–36.
- [2] Xiao H, Li H, Ou J. Modeling of piezoresistivity of carbon black filled cement-based composites under multi-axial strain. *Sensors Actuators A Phys* 2010;160(1–2):87–93.
- [3] Azhari F. Cement-based sensors for structural health monitoring. MSc. Thesis. University of British Columbia; 2008 <<http://hdl.handle.net/2429/7324>>.
- [4] Wen S, Chung DDL. Piezoresistivity-based strain sensing in carbon fiber-reinforced cement. *ACI Mater J* 2007;104:171–9.
- [5] Wen S, Chung DDL. Model of piezoresistivity in carbon fiber cement. *Cem Concr Res* 2006;36(10):1879–85.
- [6] Wen S, Chung DDL. Self-sensing characteristics of carbon fiber cement. *Proceedings of ConMat'05 and Mindess Symposium*. The University of British Columbia; 2005.

- [7] Chacko RM, Banthia N, Mufti AA. Carbon-fiber-reinforced cement-based sensors. *Can J Civ Eng* 2007;34:284–90.
- [8] Bontea DM, Chung DDL, Lee GC. Damage in carbon fiber-reinforced concrete, monitored by electrical resistance measurement. *Cem Concr Res* 2000;30:651–9.
- [9] Zhu S, Chung DDL. Theory of piezoresistivity for strain sensing in carbon fiber reinforced cement under flexure. *J Mater Sci* 2007;42(15):6222–33.
- [10] Reza F, Batson GB, Yamamuro JA, Lee JS. Resistance changes during compression of carbon fiber cement composites. *J Mater Civ Eng* 2003;15:476–83.
- [11] Chen P, Chung DDL. Carbon fiber reinforced concrete for smart structures capable of non-destructive flaw detection. *Smart Mater Struct* 1993;2:22–30.
- [12] McCarter WJ, Starrs G, Chrisp TM, Banfill PFG. Activation energy and conduction in carbon fibre reinforced cement matrices. *J Mater Sci* 2007;42:2200–3.
- [13] Han B, Guan X, Ou J. Electrode design, measuring method and data acquisition system of carbon fiber cement paste piezoresistive sensors. *Sens Actuators A Phys* 2007;135:360–9.
- [14] Chiarello M, Zinno R. Electrical conductivity of self-monitoring CFRC. *Cem Concr Compos* 2005;27:463–9.
- [15] Xie P, Gu P, Beaudoin JJ. Electrical percolation phenomena in cement composites containing conductive fibres. *J Mater Sci* 1996;31:4093–7.
- [16] Shifeng H, Dongyu X, Jun C, Ronghua X, Lingchao L, Xin C. Smart properties of carbon fiber reinforced cement-based composites. *J Compos Mater* 2007;41:125–31.
- [17] Reza F, Batson GB, Yamamuro JA, Lee JS. Volume electrical resistivity of carbon fiber cement composites. *ACI Mater J* 2001;98:25–35.
- [18] Torrents JM, Mason TO, Peled A, Shah SP, Garboczi EJ. Analysis of impedance spectra of short conductive fiber reinforced composites. *J Mater Sci* 2001;36(16):4003–12.
- [19] Shi ZQ, Chung DDL. Carbon fiber-reinforced concrete for traffic monitoring and weighing in motion. *Cem Concr Res* 1999;29(3):435–9.
- [20] Mo LT, Wu SP, Liu XM, Shui ZH. Study on the piezoresistivity character of electrically conductive asphalt concrete. In: *Proceedings of ConMat'05 and Mindess Symposium*. The University of British Columbia; 2005.
- [21] Hou TC, Lynch JP. Conductivity-based strain monitoring and damage characterization of fiber reinforced cementitious structural components. *Smart Structures and Materials: Sensors and Smart Structures Technologies for Civil, Mechanical, and Aerospace Systems*. SPIE-Int. Soc. Opt. Eng, San Diego, CA, USA; 2005. p. 419–29.
- [22] Li GY, Wang PM, Zhao X. Pressure-sensitive properties and microstructure of carbon nanotube reinforced cement composites. *Cem Concr Compos* 2007;29(5):377–82.
- [23] Senturia SD. *Microsystem design*. Boston: Kluwer Academic Publishers; 2001.
- [24] Makar JM, Beaudoin JJ. Carbon Nanotubes and their application in the construction industry. *Proceedings of 1st International Symposium on Nanotechnology in Construction*. Paisley, Scotland; 2003.
- [25] Raki L, Beaudoin J, Alizadeh R, Makar J, Sato T. Cement and concrete nanoscience and nanotechnology. *Mater Open Access J* 2010;3:918–42. <http://dx.doi.org/10.3390/ma3020918>.
- [26] Gengying L, Peiming W. Microstructure and mechanical properties of carbon nanotubes-cement matrix composites. *J Chinese Ceram Soc* 2005;33(1):105–8.
- [27] Yazdanbakhsh A, Grasley Z, Tyson B, Abu Al-Rub RK. Distribution of carbon nanofibers and nanotubes in cementitious composites, transportation research record. *Journal of the Transportation Research Board*, No. 2142, Transportation Research Board of the National Academies, Washington, D.C.; 2010, p. 89–95.
- [28] Banthia N, Djeridane S, Pigeon M. Electrical resistivity of carbon and steel micro-fiber reinforced cements. *Cem Concr Res* 1992;22:804–14.
- [29] Monfore GE. The electrical resistivity of concrete. *J PCA Res Dev Lab* 1968;10(2):35–48.